

LONG-WAVE MITIGATION STUDY FOR THE PORT OF NGQURA

Christophe Troch¹, Luther Terblanche², Marius Rossouw², Zanele Ntantala³ and Gerrit du Plessis³

Solutions to the long-wave induced moored ship motion problems at the Port of Ngqura were investigated in this study. Long-wave mitigation options were modelled with various layout modifications to the present model of the port, which has been validated with measured data. The numerical model simulations were used to derive long-term data sets inside the Port. Several moored ship motion simulations, using alternative conventional and dynamic mooring options, were performed for an extreme wave and wind condition for each berth at the port. Preferred port layout options and optimal mooring solutions were then determined for each berth. A complete framework of wave and ship motion simulations were performed for the preferred mitigation options. The ship motions and mooring line forces were determined for the relevant vessels at selected berths. This allowed for berth operability and downtime statistics to be determined, taking the limiting wave height and allowable mooring line criteria into account. Since several port layout options and different mooring arrangements were assessed, a Multi-Criteria-Analysis (MCA) was followed to determine the best possible solution.

Keywords: long-waves; mitigation; port layout; moored ship response; numerical modelling; downtime; operability

INTRODUCTION

The Port of Ngqura is situated in Algoa Bay, about 20 km northeast of Port Elizabeth, South Africa. Operations commenced in 2009, and it is the newest of the South African ports. Originally planned as a bulk port, the port has been adapted for container handling. Ngqura's current primary role is to target transshipment cargoes for the East and West African ports, as well as inter-continental transshipments. The port is, however, being prepared to take over the oil terminal from the nearby Port of Port Elizabeth. The manganese export operation, presently at Port Elizabeth, is also planned to be moved to Ngqura. Thus, significant growth is planned for the Port of Ngqura.

The port experience problems with moored container vessels. Under certain environmental conditions, these moored vessels experienced large motions, which lead to reduced operability or downtime and sometimes mooring line failures. One of the main contributing factors to the mooring problems are long-waves (Rossouw et al., 2013), which induce basin and moored vessel resonance. The port has, over the years, investigated ways to improve the mooring conditions at the container quays. Several studies have been undertaken to quantify the occurrence and predictability of long waves and their impact on moored vessels at the port (Terblanche and van der Molen, 2013).

As part of the FEL2 development for the Port of Ngqura, an additional mitigation study was undertaken to identify solutions to the excessive motions of moored container vessels as a result of the infragravity or long-waves. The study also aimed to improve operational safety and to minimise the risk imposed by the excessive low-frequency vessel movements induced by these infragravity waves.

GENERAL APPROACH

Due to the extent of the project, a phased approach was followed. In phase 1, a wide range of options with changes to the port layout was assessed. The aim was to reduce the long-wave heights inside the port. Phase 2 consisted of more detailed numerical wave modelling of selected layout options from phase 1. The wave climate at selected berths was derived for a detailed evaluation of the long-wave heights at each berth. The models were also validated with an extensive measured wave data set. For phase 3, a moored ship response study at the berths for different vessels was conducted for various alternative conventional mooring layouts, including shore-based hydraulic tensioning systems and an automated vacuum mooring system. The mooring layouts with the best performance in reducing the effect of the long-waves on the moored vessels were then identified. In phase 4, the selected mooring layouts from phase 3 was modelled with the complete wave climate for the port layouts identified in phase 1. The operability and downtime for vessel operations at the berths, considering the limiting

¹ Council for Scientific and Industrial Research (CSIR), 10 Jan Celliers Rd, Stellenbosch, 7600, South Africa

² WSP Group Africa, Portswood Rd & Beach Rd, Victoria & Alfred Waterfront, Cape Town, 8001, South Africa

³ Transnet Port Authority, Neptune road, Port of Ngqura, Port Elizabeth, 6100, South Africa

criteria of ship motions and forces, were then determined for the selected layout options. The flow diagram illustrated in Figure 1 outlines the approach adopted. Each phase is discussed in the proceeding sections.

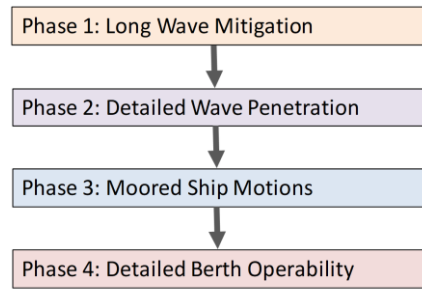


Figure 1. Flow diagram of the phased approach to study.

PHASE 1: LONG-WAVE MITIGATION

Model Setup

To predict the infragravity wave field near a berth accurately for a given wave condition at deep water, it is required that all relevant wave propagation and inter-frequency energy transfer processes are taken into consideration in the modelling process. The nonlinear long-wave modelling tool Delft3D-Surfbeat (Reniers et al., 2001, 2004), takes these processes into account and was used in this study.

A nested SWAN model, consisting of three grids, was set up to compute the swell wave propagation inside the bay (Terblanche and van der Molen, 2013). The extent of each of the grids is shown in Figure 2. Each nested grid has a finer resolution and the ability to resolve the swell waves in more detail.

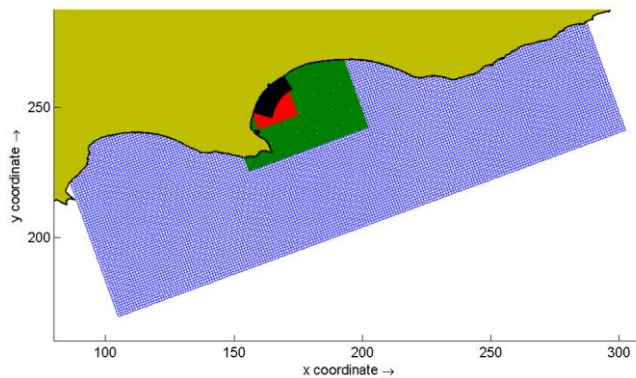


Figure 2. The extent of each grid used for the models where the coarse, medium and fine SWAN grids are indicated by blue, green and red, respectively and the Surfbeat grid is indicated in black.

The offshore SWAN grid extends approximately 60 km offshore, and is approximately 210 km wide. A second SWAN grid covers the bay and is approximately 50 km wide, and extends 30 km offshore, while the smallest SWAN grid covers the area around the port.

The output of the SWAN model serves as input and boundary conditions for the Surfbeat model to compute the propagation of the bound long-waves generated by the swell wave groups. The Surfbeat curvilinear grid is nested inside the fine SWAN wave grid. The location of the Surfbeat grid is shown in black in Figure 2.

The offshore boundary of the Surfbeat model is situated at the 28 m depth contour, approximately 7 km offshore. The model domain covers approximately 20 km of coastline to include the effects of long-waves reflecting from the beach. The model bathymetry included the latest bathymetrical surveys.

Boundary Conditions

A typical winter storm swell wave condition of 2.7 meters, 16 seconds and 144 degrees measured at the Datawell Waverider buoy, positioned about 2.5 km south-east of the port entrance, was used to

analyse the changes in the long-waves inside the port. This wave condition was used for all the layout simulations in phase 1.

Layout Changes

The layout changes or modifications were developed in consultation with the port engineer. A selection of the layout options tested, together with their intended purpose, is summarised in Table 1. The associated bathymetry layouts are presented in Figure 3.

Table 1. The layout options simulated.

Layout	Description
(a)	The base layout / short term layout.
(b)	Extension of the main breakwater with 1000 m in an attempt to reduce the long-wave energy entering the port.
(c)	Opening of an area behind the basins, the basins here were extended about 60 m inland and 70 m of the quay was removed. This forms a channel with a width of about 130 m. The idea here was to let the long wave energy move more freely behind the two basins.
(d)	The opening of the salt works behind the port for 1.7 km inland with a depth of 1 m CD, so that the energy can move through the port and dissipate in the salt works area.
(e)	Construction of 4 channels or culverts each with a width of 10 m at the back of the western basin. The length of these channels ranges between 750 – 950 m. The channels start with a depth of 10 m and gradually rises to a depth of 1 m over a length of 130 m. This was more of a theoretical approach where the channels are used to dissipate the long-wave energy.
(f)	The same as layout option (e), but also removing part of the quay to form a connecting channel with a width of 90 m, similar to layout option (c).

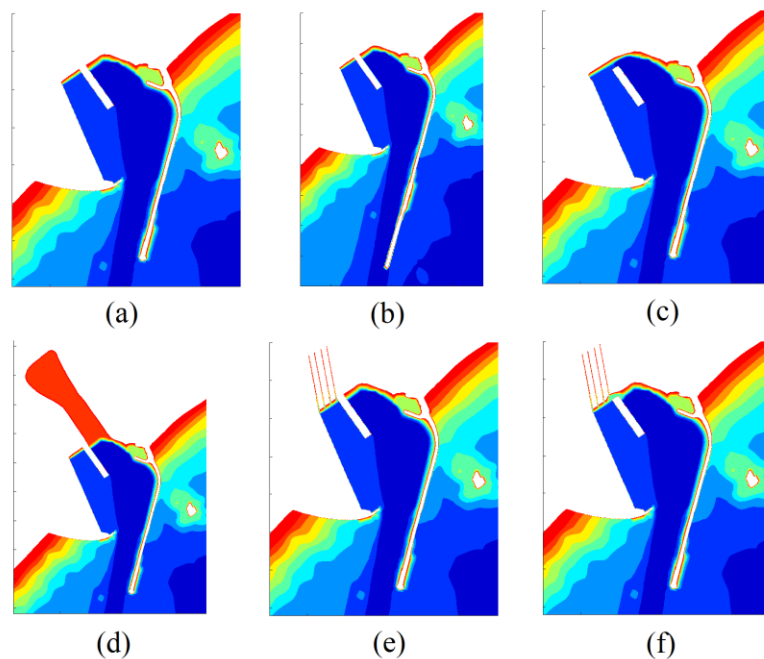


Figure 3. The layout options tested as described in Table 1.

The same typical winter storm boundary condition was used as input to the model for each of the layout options. From the simulations, the spatial percentage change in the significant long-wave height for each layout option, relative to the wave height for the current layout, could be calculated. The contour plots showing the differences are presented for each layout in Figure 4, the base layout with

zero percentage change is also shown for illustrative purposes. The percentage reduction or increase in wave height follows the colour scale. For example, the blue colour indicates a reduction in wave height, while the red indicates an increase in wave height. Green indicates no to very little change. The base layout together with two alternative options (d) and (e) was modelled in more detail and is discussed later.

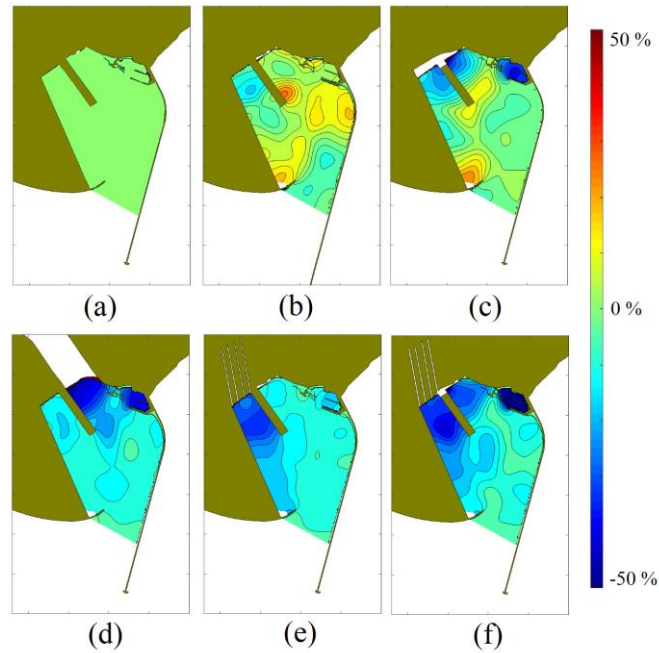


Figure 4. The spatial percentage change in significant long wave height for the layout options relative to the base layout, as described in Table 1.

PHASE 2: DETAILED WAVE PENETRATION

Modelling Approach and Setup

Although the main focus of this study was the setup and modelling of the long-waves inside the port, a numerical model for the short-waves or swell entering the port was also set up. The MIKE 21 Boussinesq Waves (BW) was applied to model the short-waves. It is worth noting that the short-waves are defined by waves with a period of about 5 s to 25 s. The long-waves cover the period range between 25 s and 350 s.

The numerical models were calibrated using the present port layout with wave measurements collected at various locations inside and outside the port. The instrumentation included RBR pressure sensors and ADCP measurements for 3 months, a water level recorder (LWR) for 5 years and Waverider buoy for approximately 7 years. Another ADCP was deployed just outside the port entrance. Following the calibration of the present layout model, the same boundary conditions were applied to the base layout and two selected alternative model layouts of the port. The Surfbeat model was calibrated against measured long-wave data at the ADCP, LWR and RBR locations with the measured short-wave data recorded at the Waverider buoy and ADCP outside the port. A selection of storm events was chosen from overlapping measurement periods for calibration purposes.

Calibration of the model was obtained by running a SWAN simulation with offshore boundary conditions such that the computed swell spectrum and wave height at the measurement location matched the measured swell spectrum and significant wave height as closely as possible. A series of Surfbeat runs were then carried out with variations in the user defined parameters to obtain a good representation of the measured significant long-wave height and spectrum. The parameters were chosen such that the short-wave energies as computed in Surfbeat correlates well with the short-wave heights computed with SWAN over varying water depths.

Long Wave Model Validation

The long-wave model was validated with the RBR, ADCP and LWR long-wave measurements. This was done by performing a total of 24 Surfbeat runs which correspond to different swell wave conditions at the Waverider. The 24 runs comprised 3 significant wave heights, 4 peak periods and 2 peak wave directions. The model output of the 24 Surfbeat runs forms a framework for an interpolation scheme at each model output location. This framework can be used to transform swell waves measured at the Waverider into modelled long-waves at any of the model output locations. Using this approach, a sufficiently long data set of long-waves could be generated for statistical analyses.

By applying the interpolation scheme to the RBR, ADCP and LWR model output locations, the measured and modelled long-waves could be compared. The time series of modelled and measured long-waves at the LWR location are shown in Figure 5.

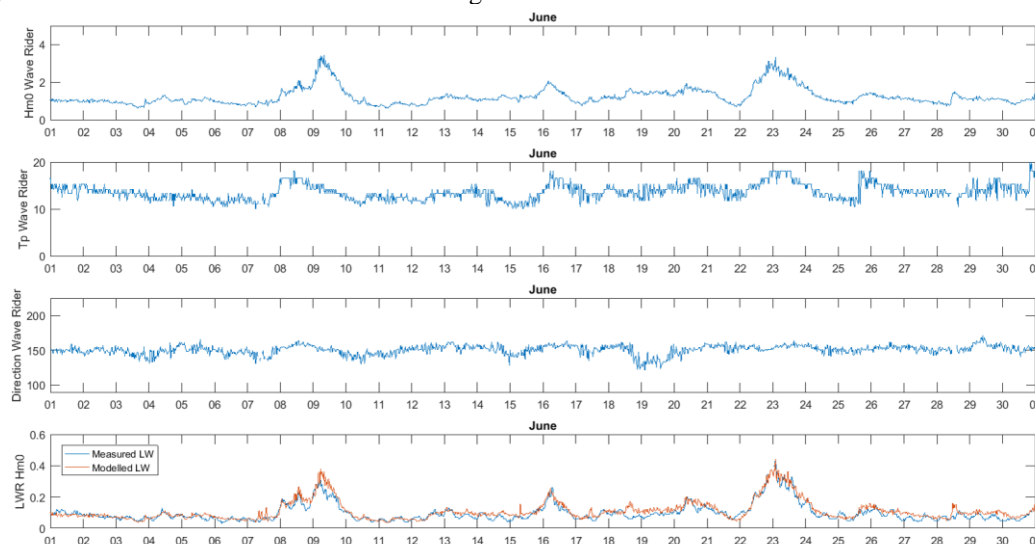


Figure 5. Time series of the modelled and measured significant long-period wave height for 1 month.

The exceedance curves of the measured and modelled long-waves at the LWR location is presented in Figure 6. The model and measured long-waves at the LWR compare well and are statistically representative of each other. It should be noted that only the LWR data from 2015 to 2017 was used, this was done to minimise the effect the changes in the port, in recent years, could have had on the long-wave climate inside the port.

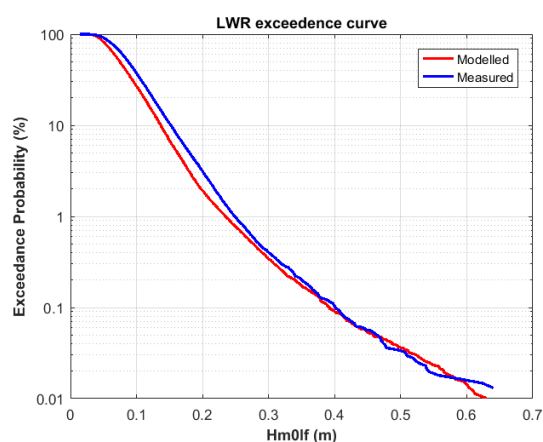


Figure 6. The measured and modelled exceedance curve for the long-wave recorder inside the port for the period 2015 to 2017.

Long-Wave Model Output

Applying the same framework of boundary conditions from the present layout to the short term/base layout, and the selected two alternative layouts, a wave climate for the layouts were determined.

The semi-enclosed port basin has natural frequencies which can be enhanced when long-waves enter the port. If the natural period of the moored vessel is close to the frequencies where energy focusing occurs, excessive vessel motions can be induced. Natural resonance periods of moored vessels are typically in the order of 50-100 s for a medium-sized vessel with a stiff mooring system but can be up to 300 s for large vessels with a very elastic mooring system. The next phases of the study will show what effect these focusing and shifts of energies will have on the different moored vessels at the various berth locations.

Exceedance Curves of Long-Waves

The model output consisted of a time series of low-frequency water elevations (the modelled long-waves). The time series at each of these output locations were analysed to determine a significant long-wave height for each of the 24 modelled run conditions in the runs framework.

The swell data from the Waverider buoy (2011-2017) was used to calculate the corresponding long-wave heights at the berth locations. A long-wave time series was then calculated at each berth location and the long-wave climate at each of the berth location for each layout was determined.

An example of the exceedance values (long-wave heights) for one of the container terminal berths, for the short term/base layout and the two alternative options, are presented in Figure 7.

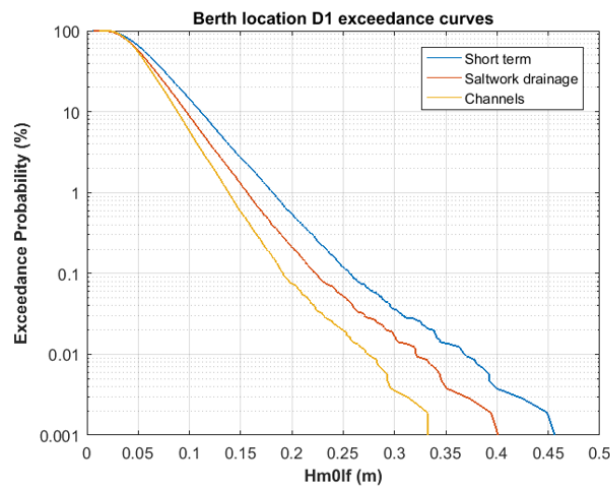


Figure 7. The significant long-wave height exceedance curves for the various layouts at one of the container berths.

Extreme Long Wave Heights

The extreme long-wave heights were estimated for each berth location using an extreme statistical analysis. To estimate the extreme long-wave heights, a 3-parameter Weibull distribution was fitted to a selection of the wave height data using the Peaks-over-Threshold (POT) method (Goda, 2010; Holthuijsen, 2010). The Weibull function was fitted using the Least-squares method. The estimations were done using a procedure whereby the optimum threshold (POT) level was selected (Thompson et al., 2009).

A time series of modelled significant wave heights at 9 berth locations inside the port were analysed to determine the return conditions. This analyses illustrated the effect more extreme storm events would have on the different port layouts. It should be noted that the Waverider data (2011-2017) was used for this analysis, a longer data set would be required to give a more accurate statistical representation.

PHASE 3: MOORED SHIP MOTIONS

Modelling Approach and Setup

In most detailed mooring analysis studies, a time-domain simulation model is used to determine the motions of the moored ship and the loads in the mooring lines. These models solve the equations of motion of the ship in the time-domain, so that nonlinearities, such as the characteristics of fenders and mooring lines, drift forces and current forces, can be accommodated. A pre-calculated hydrodynamic file was used, which includes the hydrodynamic coefficients and first and second order wave force transfer functions. This hydrodynamic file was generated using a panel model to represent the 3D shape of the ship hull, the quay and the sea bed and is based on 3D diffraction theory. After this file has been obtained, quick computations can be carried out to determine the response in a different wave, current and wind condition or for different configurations of the mooring layout.

Wave Forces Acting on the Vessel

The swell waves are included in the moored ship program Quaysim (van der Molen et al., 2016). The swell wave input parameters are determined using the MIKE 21 Boussinesq Waves (BW) rectilinear model.

Although the description of bound long-waves is included in the moored ship program Quaysim, this only applies for the situation where these waves are still bound to the wave groups and the moored vessel is in open water. Where these bound long waves become free long-waves, such modelling of the free long-waves is not directly included in Quaysim and has to be computed using other appropriate models such as Surfbeat. Due to the presence of the breakwater and the reflections on the shoreline and inside the harbour basin, Quaysim cannot be used alone to assess the long-wave forces acting on the moored vessel. Instead, the approach has been followed to assess the bound and free long-wave forces acting on the vessel externally and include the computed forces as an external force file in the computation of the dynamic vessel response.

The long-wave forces on a moored ship are determined with the model LF-Strip (Van der Molen, 2003; Van Der Molen et al., 2006), developed at the Delft University of Technology. The model calculates the forces directly from the long-wave elevations and fluid motions as obtained with Surfbeat. LF-Strip is based on strip theory, i.e. the submerged ship hull is divided into 20 cross-sectional strips and the force per cross-section is calculated with the assumption that the section is part of a long cylinder. Integration of the cross-sectional forces yields the total force on the ship.

For the determination of the diffraction part of the wave force (where the ship modifies the incident waves), the model uses the relative motion principle, which relates the diffraction force to the fluid motions and the hydrodynamic coefficients. These coefficients are provided from Quaysim's hydrodynamic file as obtained with the panel model Wavescat (van der Molen et al., 2016, 2010). This hydrodynamic computation includes the effect of a (partially) reflecting quay wall near the ship. Hence, despite the use of a 2D strip theory method, the diffraction analysis uses coefficients obtained with 3D diffraction theory.

Dynamic Mooring Analyses

The berths inside the Port of Ngqura are protected by breakwaters. These breakwaters and the approach channel transform the wave field and long-waves, including those reflected from the shore. The breakwaters, therefore, have a considerable effect on the waves and associated ship motions inside the port. They provide protection from short-waves, swell and to some extent long-waves induced by wave groups. Harbour oscillations can be generated which can have detrimental effects on the behaviour of ships moored in the port. Therefore, special focus is placed at the propagation of long-waves into and inside the port and their effects on the moored ships.

The time domain Quaysim computer program, capable of analysing the dynamic behaviour of a moored ship subject to wind, waves and current, is used in this study. The program predicts the mooring loads and ship motions when the system is exposed to operational environmental conditions.

Moored Vessel Setup

The Port of Ngqura is equipped with different fenders for specific berths. The reaction force as a function of deflection for the fenders used in the port was used as input to the model, which include Unit Element, tyre and pneumatic fenders. The mooring line type used is vessel dependent, various elongation curves of the mooring lines were used in this study as input to the model.

The vessels used in the numerical dynamic mooring analyses are a 9 000 TEU container vessel, a 100 000 DWT bulk carrier and a 70 000 DWT bulk carrier. The design dimensions of the vessels are given in Table 2. Computations were carried out in the laden and ballast condition.

Panel meshes were generated for the vessels, based on the line drawings of a typical container and bulk carrier vessels. The panel mesh is used by the 3D panel model, Wavescat to compute the hydrodynamic properties of the vessels as well as the wave force transfer functions.

Table 2. Main dimensions of the vessels.				
Vessel		9000 TEU	100 000 DWT	70 DWT
Displacement (laden)	[t]	142 470	129 913	101 458
Length-over-all	[m]	352	263	229
Beam width	[m]	42.8	42.5	40.1
Draught (laden)	[m]	14.5	15.4	13.8
Draught (ballast)	[m]	9.5	6	6
Depth	[m]	28	22.9	18.8
Block coefficient (laden)	[-]	0.67	0.79	0.82

Mooring arrangements and systems

Various mooring arrangements were tested for each berth and vessel, this included various alternative conventional mooring layouts with changes to the line types, e.g., polypropylene, polyolefin and Dyneema®. Various mooring line patterns were also tested with changes to the number of mooring lines, line length and pretension ranging from 10% to 20% of the Minimum Breaking Load (MBL) of the line. The MBL of the lines generally used for the size and type of vessel under consideration was implemented.

The automated mooring systems that were simulated includes a land-based hydraulic tensioning system and a vacuum mooring system. The hydraulic tensioning system has a hydraulic head that can move backwards and forwards to increase or decrease tension in the mooring lines. The speed at which the head moves is determined by the level of tension in the line. The head is set to move such that the tension in the line does not exceed 600 kN. One Dyneema® line was used to connect the tensioning system to the vessel regardless of the other mooring lines used by the vessel, a combination of 2 and 4 units was assessed. The automated vacuum mooring system is modelled by 22 x 200 kN units, stacked in pairs and placed between the fenders, spaced 20 m apart. The vacuum system reacts quickly to movements and generates high horizontal forces on very small motions, making it a very stiff system. This influences the natural frequency of the system, thereby making it a very efficient mooring system to control movements of moored vessels

An example of the mooring arrangement for a container vessel moored with 4 hydraulic tensioning units at one of the container berths is presented in Figure 8. The units are indicated by the green squares and the fenders are shown as blue squares. The mooring legs are represented by the red lines, mooring legs 1, 2, 7 and 8 consists of 2 polypropylene lines each whereas mooring legs 3, 4, 5 and 6 consist of 1 Dyneema® line each.

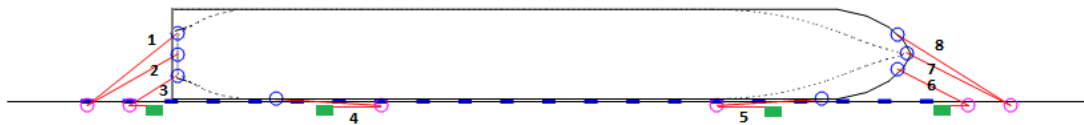


Figure 8. The mooring layout for a container vessel with 4 hydraulic tensioning units.

Environmental Conditions

The long- and short-period waves in the Port of Ngqura have been calculated with Delft3D-Surfbeat and the MIKE 21 (BW) model for 24 incident swell wave heights and peak periods.

It can be concluded that the berths are reasonably well protected against the incoming swell by the main breakwater. Therefore, it appears that the diffraction of the swell around the breakwater, as determined by the Mike21 model, does not play a dominant role in the forcing on the ship. The long-waves associated with the incoming swells diffract more due to the larger wavelength of these waves. Moreover, the long-waves do not fully break at the beach, but partially reflect to the ocean and into the port entrance. These forces dominate the forcing on the moored ships. The combined forces resulting from the long-waves and swell waves are used in the present mooring simulation studies as independent forces.

The wave conditions in the port are related to the calculated wave height at a measurement location outside the main breakwater. The wave condition calculated for this location can be related to the occurrence percentages derived from the measured data set outside the port and can be used to calculate occurrence percentages inside the port. The extreme wave condition used for testing the different moored vessel simulations is an event with a wave height of 2 m, a period of 16 seconds and a direction of 155 degrees, measured at the location outside the main breakwater. The wave height and period has exceedance values of 0.9% and 3.2%, respectively.

Wind time series of gusting winds, with an hourly average of 15 m/s for the bulk carriers and 10 m/s for the container vessels, were generated according to a Harris-DNV spectrum. Time series of wind force coefficients are obtained from the work of Yamano (Yamano, 1997) for input to the moored ship simulations. The generated time series of wind velocities are then applied to the vessel. The 10 m/s hourly average wind speed is below the limiting wind speed where the STS cranes can operate (their operational limit is about 22 m/s). For all the simulations the wind was assumed to be from a westerly as well as an easterly direction. The westerly wind direction is the most severe wind direction for moored container vessels at the Port of Ngqura since it can push the vessel from the fenders, reducing the effect of fender friction and directly increasing the tension in the mooring lines.

The 10 m/s easterly and westerly wind corresponds to a 4.1% and 5% exceedance value, respectively. The 15 m/s easterly and westerly wind corresponds to a 0.4% and 1% exceedance value, respectively. For the easterly wind, the ENE, E and SSE sectors are combined and for the westerly wind, the WSW, W and WNW sectors are combined. Wind speeds and directions are measured at the main breakwater. It is accepted that the location of the wind station on the main breakwater, in the open sea, is slightly more exposed than the terminals in the Port of Ngqura. This probably renders the tested conditions slightly conservative.

It is assumed that currents at the berths inside the Port of Ngqura are negligibly small, and was therefore ignored in the present vessel motion computations.

The tide levels at the Port of Ngqura range between 0 m CD (LAT) and +2.12 m CD (HAT). All simulations were done at Mean High Water Neap tide (MHWN), which is at +1.3 m CD.

Layouts

The moored ship simulations were conducted for the base/short term layout (a), the salt work layout (d) and the 4 channel layout (e) as presented in Figure 4. These layouts were identified to be possible implementable options from phase 2 of the study.

PHASE 4: DETAILED BERTH OPERABILITY

Limiting Criteria for Operability

The computed significant ship motions and maximum mooring line forces under operational conditions are compared with the criteria for the container and bulk terminals to determine the limiting wave conditions. The following subsections present the criteria used to determine the limiting wave heights, which are in turn used to compute an estimate for the percentage of time when the criteria will be exceeded. This is done by integrating the occurrence percentages in the wave occurrence tables. Two sets of occurrence percentages are calculated. One set is based on the significant motion criteria where either surge or sway motions are used, depending on which one is higher. The other set is based on maximum mooring line forces or fender compression, depending on which one gives the lowest limiting wave height.

Container Vessel Motion

The criteria for maximum container vessel motions extracted from the British Standards (BSI, 2013) are shown in Table 2. These are derived from and are the same as in Table 1.2 of (PIANC, 1995). These values are accepted to be the significant peak-to-peak vessel motions and can be exceeded by 10% to 15% for short periods while remaining acceptable.

Table 2. Container vessel motion criteria.				
Motion	BS and PIANC 100 % efficiency	BS and PIANC 50 % efficiency	PIANC (2012) 100 % efficiency	PIANC (2012) 50 % efficiency
Surge [m]	1	2	0.4 m - 0.6 m	2 m - 3 m
Sway [m]	0.6*	1.2*		
Heave [m]	0.8	1.2		
Roll [°]	3	6		
Pitch [°]	1	2		
Yaw [°]	1	1.5		

* motion off fender line

The PIANC Working Group 52 on “Criteria for the (Un-)Loading of Container ships” (PIANC, 2012) determined new estimates for the 50% efficiency criteria for container vessels based on significant surge motions. These estimates were based on computer simulations by Moes and Terblanche (Moes and Terblanche, 2010). The committee assigned to update the present British Standards BS 6349 intend to include these new PIANC criteria again into their new BS standards.

One of the outcomes of the numerical study, as reported in (Moes and Terblanche, 2010), is that for an allowable container placement (pin out of hole centre) criterion of 0.1 m and a velocity of 0.05 m/s, 95% efficiency will be reached at a significant surge motion of about 0.6 m, while 50% efficiency will be reached at a significant surge motion of about 3 m (note that the figures in the PIANC report indicate surge motion amplitude, which is half the surge motion peak-to-peak range, as used in this report). For a reduced placement criterion of 0.05 m, the significant surge motions are 0.4 m for 95% efficiency and 2.2 m for 50% efficiency. If this placement criterion range of 0.05 m to 0.1 m is realistic, the new PIANC and BS surge motion tolerance will be smaller for 95% efficiency but larger for the 50% efficiency in comparison with (BSI, 2013) and PIANC (1995) criteria, as listed in Table 4-1.

The more conservative 50% efficiency criteria for significant surge and sway motions of BS 6349-1 and PIANC (1995), as shown in Table 2, are used in this study to compare the different mooring systems concerning vessel movement.

Bulk Carrier Motion

The vessel motion and force limits are primarily based on BS (BSI, 2013) and PIANC (PIANC, 1995) guidelines. The motion criteria vary and are primarily dependant on the capabilities of the loading arms that are used at the loading facility. The maximum vessel motion limits are presented in Table 3.

Table 3. Bulk carrier motion criteria.		
Motion	BS (2013)	PIANC (1995)
Surge [m]	0.5 - 2.0*	3
Sway [m]	0.5 - 2.0	3

* Loading arm and mooring force dependant

Based on Table 3, a surge and sway limit of 2.0 m will be implemented. The ship motions model is run in the time domain, thus the significant motions are often more representative of the process being modelled. The maximum motion limits in Table 3 are therefore converted to significant motion limits. In the case of horizontal ship motions of surge and sway, during a six-hour event, assuming a typical oscillation period of 60s and a Rayleigh distribution, the expected single maximum motion would be

1.72 times the significant motion (PIANC, 2012). The moored ship simulations in this study are for 4 hours, which would have an expected maximum motion of 1.65 times the significant motion. The conversion factor of 1.72 from PIANC was still used as a conservative measure. The significant motion limit is thus 1.16 m.

Mooring Line Forces

The PIANC 1995 guidelines state that the forces in steel mooring lines should not exceed 55% of the minimum breaking load during normal use, while the forces in synthetic lines should not exceed 75% of the minimum breaking load during normal use. The PIANC guidelines recommend that the mean mooring line forces should not exceed 25% of the breaking load and the repeated force should not exceed 50% of the breaking load to ensure a long life-time of the mooring ropes. In this study, a maximum mooring line load criterion of 55% has been applied for all mooring lines, even for polypropylene mooring ropes.

Fender Compression

In the absence of specific PIANC guidelines, a maximum of 75% compression of the original fender height has been applied as a limiting criterion for the unit element fenders. The tyre fenders are limited to a 40% deflection, and the pneumatic fenders at 60% compression of the original fender diameter.

Limiting Wave height and Operability

The limiting wave height is defined as the wave height for which the ship motion is equal to the limiting motion criterion or when the maximum mooring line load is 55% of the minimum breaking load (MBL) of the mooring lines or the maximum fender compression is reached.

Each wave simulation is linked to the significant surge, sway, mooring line force and fender compression. A trend line for each wave height using the limiting criterion for each wave period and direction is produced. The limiting wave height is then estimated as the intersection between the trend line and the ship motion or mooring line force criterion. The limiting wave height for wave periods in the occurrence table that were not modelled is estimated by linear regression. The values are then also weighted according to the occurrence percentages of the wave direction as based on the S4 wave data using the modelled wave directions. Limiting wave heights for the directions that were not modelled, but which are listed in the directional occurrence table of the S4 data are estimated by regression. A similar lookup table approach was applied in the long-wave modelling procedure.

The loaded and ballasted conditions of the vessels were modelled and the limiting wave heights were estimated by linear interpolation for the intermediate loading conditions. Subsequently, the wave height is related to the occurrence table of wave heights by interpolating between the provided steps of the occurrence table. In this way, operability percentages were obtained for intermediate loading conditions which could then be averaged to provide an average operability value for the particular vessel. In this process, it is assumed that the draught of the ship increases linearly in time and the limiting wave height varies linearly with the draught (or the percentage loading condition).

Operability percentages were not computed for the automated mooring systems based on forces since the same trend lines cannot be achieved. The forces are influenced by the dynamic mooring system and often capped or held more or less constant at a specified maximum force. In this case, the slope of the trend lines is flat and a limiting wave height cannot be determined.

An example of the operability percentages for ship motions associated with a threshold for which 50% loading efficiency can be achieved is presented in Table 4. The operability percentages presented is for the container vessel (C9000) moored at one of the container berths (D1) using a conventional mooring layout (M4) and also using 4 hydraulic tensioning units (M9) for each port layout option (a), (d) and (f) as described in Table 1, where no wind was present. Similarly, the downtime percentages for the vessel exceeding the criterion of 55% of the breaking load is presented in Table 5. Note the berth operability refers to the ship motions, while downtime is linked to the allowable mooring line forces, i.e. 55 % of MBL as well as the maximum fender compressions.

Table 4. Operability percentages for ship motions associated with a threshold for which 50% loading efficiency can be achieved with no wind and vessels are moored with a pretension of 10 %.

Berth	Vessel	Mooring	Layout	Ballast	←----- Loaded % -----→					Laden	AVG
				0 %	20 %	40 %	60 %	80 %	100 %		
D1	C9000	M4	(a)	98.74	98.24	97.47	96.45	94.81	92.63	96.39	
D1	C9000	M4	(d)	99.39	98.91	98.07	96.63	93.85	87.44	95.71	
D1	C9000	M4	(f)	99.18	98.75	98.06	97.10	95.70	93.42	97.03	
D1	C9000	M9	(a)	100.00	99.93	99.83	99.55	98.87	97.40	99.26	
D1	C9000	M9	(d)	100.00	99.98	99.95	99.87	99.57	99.44	99.80	
D1	C9000	M9	(f)	100.00	99.99	99.96	99.90	99.76	99.50	99.85	

Table 5. Downtime percentages for vessels exceeding the criterion of 55% of the breaking load with no wind and vessels are moored with a pretension of 10 %.

Berth	Vessel	Mooring	Layout	Ballast	←----- Loaded % -----→					Laden	AVG
				0 %	20 %	40 %	60 %	80 %	100 %		
D1	C9000	M4	(a)	0.01	0.05	0.11	0.22	0.36	0.61	0.23	
D1	C9000	M4	(d)	0.00	0.05	0.12	0.22	0.48	0.95	0.30	
D1	C9000	M4	(f)	0.01	0.03	0.07	0.15	0.24	0.35	0.14	
D1	C9000	M9	(a)	0.00	0.01	0.02	0.04	0.05	0.07	0.03	
D1	C9000	M9	(d)	0.00	0.00	0.00	0.00	0.00	0.00	0.00	
D1	C9000	M9	(f)	0.00	0.00	0.00	0.00	0.00	0.00	0.00	

MULTI-CRITERIA ANALYSES

Selected Options

A Multi-Criteria Analysis (MCA) was done taking the layout options and the various mooring arrangements into account. The process followed in this study produced a variety of options that could be evaluated. These options included the three layout options with conventional mooring layouts, the use of hydraulic tensioning systems in place and the use of an automated vacuum mooring system. These variations were tested with a mooring line pretension of 10% and 15%.

Criteria Used to Evaluate Options

A set of criteria was developed to compare the rating of the options. At this early stage of the assessment of options, there was limited detail for each option and the rating was thus interpretive. Options were rated on a scale of 1 to 3, with a low score being unfavourable (poor) and a high score being favourable (good). The criteria were developed through a collaborative approach with TNPA. A weighting was also assigned to each criterion to differentiate the relative importance or severity of the criteria.

The final criteria used included:

1. Cost such as capital cost and maintenance.
2. Implementation time.
3. Operational delays during implementation or maintenance.
4. Expansion potential.
5. Environmental effects.
6. Technological maturity.
7. Early return on investment.
8. Robustness.
9. Spare parts availability in case of an emergency.
10. The effectiveness at each berth with regards to operability and downtime.

SUMMARY AND CONCLUSIONS

Berth Operability and Downtime

The ship motion modelling study was conducted taking numerous factors into account. The two main groups or clusters of simulations refer to the pretension of the mooring lines. The study was conducted with a pretension of 10% and repeated with a pretension of 20%.

The results of the study indicated a general increase in operability with an increase in the pretension of the mooring lines, especially at the container terminal. At the western basin of the port, the changes tested (layouts and mooring arrangement) showed pretensioning with the inclusion of the hydraulic tension system improved the situation. At the eastern area of the port, the opening up of the Salt work area showed a significant improvement. The operability of the smaller bulk carrier showed the greatest improvement. This area of the port indicated even greater improvement with the hydraulic tension systems in place. The impact of extreme wind, as modelled in this study, is also noticeable on the level of operability. It should however be noted that different characteristics of the velocity-force relationship of the hydraulic system as well as the position and arrangement can be changed to optimise the efficiency of the units.

The changes to the port layout and mooring arrangements also impacted on the downtime levels (i.e. exceeding the limit on the mooring line forces). At the western basin, the long-wave action has a significant impact on mooring lines, as experienced currently in the port. The implementation of hydraulic tension systems with a 20 % pretensioning show a marked improvement. The reason being that surge is the main factor impacting on the forces in the mooring lines. The opening of the salt works and 4 channel layout shows further improvement.

At the eastern area of the port, the opening up of the salt works area is most effective in reducing the downtime. However, the mooring arrangement for this berth should be further assessed, i.e. investigate the impact on the surge and sway components of the ship motions. It is worth noting that the percentage of downtime is linked to the maximum allowable limit on the mooring lines, which is 55% of the MBL. Therefore, the force in the mooring line would be allowed to, occasionally, exceed the limit, making the downtime statistics to some extent conservative.

Multi-Criteria Analysis Outcome

A Multi-Criteria Analysis (MCA) was done, taking the port layout options and the various mooring arrangements into account. Only the fully laden state of the vessel was assessed since a vast number of permutations of options, berths and mooring arrangements were considered.

Fifteen options were assessed for three port layout options, two mooring arrangements at two pretension levels with and without the hydraulic tension systems, as well as the automated vacuum system for the container berths.

The MCA results indicated the implementation of the salt works option with an increase in mooring line pretension and the inclusion of the hydraulic tensioning system, appears to be the most attractive option. This is followed closely by a similar setup, except with a 10% pretensioning of the mooring lines. The status quo situation in the short-term with the automated vacuum mooring system appears to be the least favourable.

Given the practicality of implementing the structural changes, it does, however, appear that the hydraulic tensioning system with a pretension of 20% in the mooring lines should be investigated for the short-term option. This option can be implemented with relative ease and no impact on port operations. A trial period of testing was recommended, and since the hydraulic tensioning system is portable it can be assessed at several berths.

ACKNOWLEDGMENTS

The authors wish to thank the Transnet National Port Authority of the Port of Ngqura for supporting the project and the valuable collaboration during the study.

REFERENCES

- BSI, 2013. BS 6349-1-1: 2013. Maritime works. General. Code of planning and design for operations. BSI London, UK.
- Goda, Y., 2010. Random seas and design of maritime structures. World scientific.
- Holthuijsen, L.H., 2010. Waves in oceanic and coastal waters. Cambridge university press.
- Moes, H., Terblanche, L., 2010. Motion criteria for the efficient (Un) loading of container vessels.
- PIANC, 2012. Criteria for the (un) loading of container vessels. Report No. 115 2012.

- PIANC, 1995. Criteria for movements of moored ships in harbours. PIANC Brussels.
- Reniers, A., Roelvink, D., Dongeren, A. van, 2001. Morphodynamic response to wave group forcing, in: Coastal Engineering 2000. pp. 3218–3228.
- Reniers, A.J., Roelvink, J.A., Thornton, E.B., 2004. Morphodynamic modeling of an embayed beach under wave group forcing. Journal of Geophysical Research: Oceans 109.
- Rossouw, M., Terblanche, L., Moes, J., 2013. General characteristics of long waves around the South African coast, in: Coasts and Ports 2013: 21st Australasian Coastal and Ocean Engineering Conference and the 14th Australasian Port and Harbour Conference. Engineers Australia, p. 653.
- Terblanche, L., van der Molen, W., 2013. Numerical modelling of long waves and moored ship motions, in: Coasts and Ports 2013: 21st Australasian Coastal and Ocean Engineering Conference and the 14th Australasian Port and Harbour Conference. Engineers Australia, p. 757.
- Thompson, P., Cai, Y., Reeve, D., Stander, J., 2009. Automated threshold selection methods for extreme wave analysis. Coastal Engineering 56, 1013–1021.
- Van der Molen, W., 2003. Long-period wave forces on a moored ship in a harbour using a strip theory approach, in: Proc. 2nd Int. Conf. on Port and Maritime R&D and Technology (Singapore), 2003. pp. 113–120.
- Van Der Molen, W., Monardez, P., Van Dongeren, A.P., 2006. Numerical simulation of long-period waves and ship motions in Tomakomai Port, Japan. Coastal engineering journal 48, 59–79.
- van der Molen, W., Rossouw, M., Phelps, D., Tulsi, K., Terblanche, L., 2010. Innovative technologies to accurately model waves and moored ship motions.
- van der Molen, W., Scott, D., Taylor, D., Elliott, T., 2016. Improvement of mooring configurations in Geraldton Harbour. Journal of Marine Science and Engineering 4, 3.
- Yamano, T., 1997. An estimation method of wind force acting on ship's hull. Journal of the Kansai society of naval architects, Japan 228.